Hydrodynamic 2D Turbulence and Spatial Beam Condensation in Multimode Optical Fibers

E. V. Podivilov,[1,2] D. S. Kharenko,[1,2] V. A. Gonta,[1] K. Krupa,[3] O. S. Sidelnikov,[1,4] S. Turitsyn,[1,5]
M. P. Fedoruk,[1,4] S. A. Babin,[1,2] and S. Wabnitz[1,6]

[1]*Novosibirsk State University, Novosibirsk 630090, Russia*
[2]*Institute of Automation and Electrometry SB RAS, 1 academican Koptyug avenue, Novosibirsk 630090, Russia*
[3]*Dipartimento di Ingegneria dell'Informazione, Università di Brescia, Via Branze 38, 25123 Brescia, Italy*
[4]*Institute of Computational Technologies SB RAS, Novosibirsk 630090, Russia*
[5]*Aston Institute of Photonic Technologies, Aston University, Birmingham B4 7ET, United Kingdom*
[6]*Dipartimento di Ingegneria dell'Informazione, Elettronica e Telecomunicazioni,
Sapienza Università di Roma, Via Eudossiana 18, 00184 Roma, Italy*

We show that Kerr beam self-cleaning results from parametric mode mixing instabilities that generate a number of nonlinearly interacting modes with randomized phases—optical wave turbulence, followed by a direct and inverse cascade towards high mode numbers and condensation into the fundamental mode, respectively. This optical self-organization effect is an analogue to wave condensation that is well known in hydrodynamic 2D turbulence.

Spatiotemporal light beam dynamics in multimode optical fibers (MMFs) has emerged in recent years as a fertile research domain in nonlinear optics [1,2]. Intriguing spatiotemporal wave propagation phenomena such as multimode optical solitons [3] and parametric instabilities leading to ultra-wideband sideband series [4], although predicted quite a long time ago, have only been experimentally observed in MMFs in the last few years [1,2,5,6].

It is well known that linear wave propagation in MMFs is affected by random mode coupling, which leads to highly irregular speckled intensity patterns at the fiber output, even when the fiber is excited with a high quality, diffraction limited input beam. Recent experiments [6–9] have surprisingly discovered that the intensity dependent contribution to the refractive index, or Kerr effect, has the capacity to counteract such random mode coupling in a graded index (GRIN) MMF, leading to the formation of a highly robust nonlinear beam. The self-cleaned beam at the fiber output has a size that is close to the fundamental mode of the MMF, and sits on a background of higher-order modes (HOMs). Typically, spatial self-cleaning is observed in several meters of GRIN MMF at threshold power levels of the order of few kWs, orders of magnitude lower than the value for catastrophic self-focusing. Moreover,

self-cleaning is most easily observed in a quasicontinuous wave propagation regime (i.e., by using subnanosecond pulses), so that dispersive effects can be neglected [6,7, 9–11]. In such a regime, nonlinear mode coupling is the sole mechanism responsible for the self-cleaning of the transverse spatial beam profile at the fiber output [12]. So far, although different tentative explanations have been provided [7,9,13,14], the physical mechanism leading to Kerr beam cleaning remains an open issue.

In this Letter, we introduce a new concept, solving this critical outstanding problem. We experimentally demonstrate that spatial beam self-cleaning in MMFs is fully analogous to hydrodynamic 2D turbulence, where a large-scale condensate (e.g., a hurricane, Jupiter's red spot, etc.) results from parametric instabilities leading to a spatial mode redistribution process. As first outlined by Kraichnan [15,16], the key ingredient of hydrodynamic 2D (as opposed to Kolmogorov's 3D) turbulence is the simultaneous presence of a direct energy cascade towards high wave numbers, accompanied by the inverse cascade towards low wave numbers and, ultimately, the condensate. Crucially, both direct and inverse energy cascades concur in conserving the average mode number throughout the whole process of development of the 2D turbulence. This is counterintuitive, as the occurrence of condensation (or beam-self-cleaning) would lead one to expect a significant reduction of the average mode number. We present, we believe for the first time, a direct experimental demonstration of the conservation of the average mode number in the process of spatial beam cleaning. By linking the phenomenology of hydrodynamic turbulence in 2D fluids

to that of transverse nonlinear optics in multimode fibers, we provide a fascinating connection that will be of special appeal to a wide physics community. Moreover, cross fertilization from the hydrodynamic approach and complex transverse spatial pattern formation in multimode optical fibers will pave the way for substantial progress in this emerging field of research, and could shed new light on other phenomena, such as spatial mode cleaning of beam filamentation in air [17,18].

The equation for the field amplitude $E = A(z, \vec{r}) \times \exp(i\omega t - ikz)$ in a GRIN fiber [with refractive index $n(z, \vec{r}) = n_0 \sqrt{1 - \Delta^2 r^2} + n_2 I + \delta n(z, \vec{r})$] reads as

$$-2ik\frac{dA}{dz} + \frac{d^2A}{d\vec{r}^2} - k^2\Delta^2 r^2 A$$
$$= -2k^2(n_2/n_0)|A|^2 A - \frac{d^2A}{dz^2} - k^2[2\delta n(z, \vec{r})/n_0]A, \quad (1)$$

where Δ is the mode spacing, $k = 2\pi n_0/\lambda$ is the wave vector, and λ is the wavelength. Terms in the right-hand side denote nonlinearity, angular dispersion, and random refractive index fluctuations. $|A|^2 = I$ is the intensity of the light beam, and all terms in the right-hand side are supposed to be small. Let us introduce the following dimensionless and normalized variables

$$\vec{\rho} = \vec{r}/r_0, r_0 = 1/\sqrt{k\Delta}, \quad \zeta = z\Delta,$$
$$\delta(z, \vec{r}) = [2k\delta n(z, \vec{r})/\Delta n_0], \quad A = \Psi\frac{\sqrt{P}}{r_0},$$
$$p = \int |A|^2 d^2\vec{r}/P_{sf} = (P/P_{sf})\int |\Psi|^2 d\vec{\rho}^2 = (P/P_{sf}),$$

where $P_{sf} = n_0/2n_2k^2 \simeq 1MW$ is the power threshold for catastrophic self-focusing. The equation for the normalized envelope Ψ reads as

$$2i\frac{d\Psi}{d\zeta} = \frac{d^2\Psi}{d\rho^2} - \rho^2\Psi + D\frac{d^2\Psi}{d\zeta^2} + p|\Psi|^2\Psi + \delta(z, \vec{r})\Psi, \quad (2)$$

where $D = \Delta/k = \lambda/2L_B \ll 1$ is the angular dispersion coefficient. The normalized field envelope reads as

$$\Psi(\zeta, \vec{\rho}) = \sum_{m,p=0}^{\infty} B_{p,m}(\zeta) U_{p,m}(\vec{\rho}) e^{i(n+1)\zeta}, \quad (3)$$

where

$$U_{p,m}(\vec{\rho}) = N_{p,m}\rho^{|m|} L_p^{|m|}(\rho^2) e^{-\rho^2/2} e^{im\phi}.$$

Here $L_p^{|m|}$ are Laguerre polynomials, $U_{p,m}(\vec{\rho})$—normalized on unity transversal eigenmode, $N_{p,m}$—normalized coefficient, and $n = 2p + |m|$. By inserting Eq. (3) into Eq. (2), one obtains equations for the complex amplitudes $B_{p,m}$.

After keeping only resonant four-wave mixing (FWM) terms, which do not rapidly oscillate with a beat length $z = L_B = \pi/\Delta$, one obtains

$$2i\frac{dB_{p,m(\zeta)}}{d\zeta}$$
$$\equiv D(n + 1)^2 B_{p,m}$$
$$+ p\sum_{m+m_1=m_2+m_3}\sum_{p+p_1=p_2+p_3} f_{p,p_1,p_2,p_3}^{m,m_1,m_2,m_3} B_{p_1,m_1}^* B_{p_2,m_2} B_{p_3,m_3}$$
$$+ \sum_{m_1,p_1} C_{m,m_1}^n(\zeta) B_{p_1,m_1}\delta(2p_1 + |m_1| - 2p - |m|). \quad (4)$$

An important physical insight into the mechanism for Kerr beam self-cleaning can be gained by neglecting random linear mode coupling, and truncating the coupled-mode equations (4) to the first three transversal modes only [19], including the fundamental mode [i.e., we set $m = 0$, $p = 0, 1, 2$ in Eq. (4)]. Let us define $A_p \equiv B_{p,0}$, where $A_i \equiv \sqrt{I_i}\exp(i\phi_i)(i = 0, 1, 2)$. One obtains the conservation laws $I_0 + I_1 + I_2 = 1$, and $I_0 - I_2 \equiv \alpha = \text{const}$, which provide the relations $I_{0,2}(\zeta) = (1 - \eta \pm \alpha)/2$, where $I_1(\zeta) \equiv \eta < 1$.

From the truncated mode amplitude equations [see Eqs. (1) of the Supplemental Material [20]], we obtain evolution equations for the normalized power η of the intermediate transversal mode with $(m = 0, p = 1)$ and the phase $\theta = \phi_0 + \phi_2 - 2\phi_1$ in compact Hamiltonian form

$$\frac{d\eta}{d\xi} = \frac{dH}{d\theta}, \qquad \frac{d\theta}{d\xi} = -\frac{dH}{d\eta}, \quad (5)$$

where $H = H_T \cos(\theta) + H_S$, $H_T = \eta\sqrt{(1 - \eta)^2 - \alpha^2}$, $H_S = (q - K_1)\eta + K_2\eta^2$, $\xi = p\zeta/8$, and $q = 32D\pi/p$, with constant coefficients K_1 and K_2 as defined in the Supplemental Material [20]. Equations (5) have saddle points $\eta_e = 1 - |\alpha|$ and $\eta_e = 0$ at large q. In the linear limit (i.e., for $p \ll D$, or sufficiently large q), the linear wave vector mismatch suppresses the FWM-induced energy exchange between transversal modes.

A bifurcation of the saddle points occurs when new maximum (or minimum) of $H(\theta, \eta)$ appears on the phase diagram. Namely, when $dH/d\theta = 0$, and $dH/d\eta = 0$. For the detailed discussion of the bifurcation conditions of the saddle points, again we refer to the Supplemental Material [20]. The consequence of the parametric instability in the dynamics of the spatial mode coupling process can be easily visualized with the help of phase plane portraits (i.e., constant level curves of the Hamiltonian H) of the solutions of Eqs. (5), as illustrated in Fig. 1. As can be seen, when diffraction dominates over FWM (e.g., when $q = 4$), the modes virtually do not exchange energy but only experience a relative phase rotation. On the other hand, at high input power p, (e.g., with $q = 0.5$), the intermediate mode with $(m = 0, n = 1)$ can get fully depleted. Moreover, a
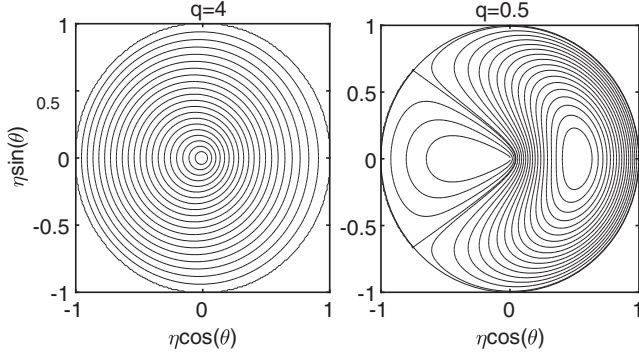
FIG. 1.   Phase plane portraits for $q = 4$ and $q = 0.5$, with $\alpha = 0$.

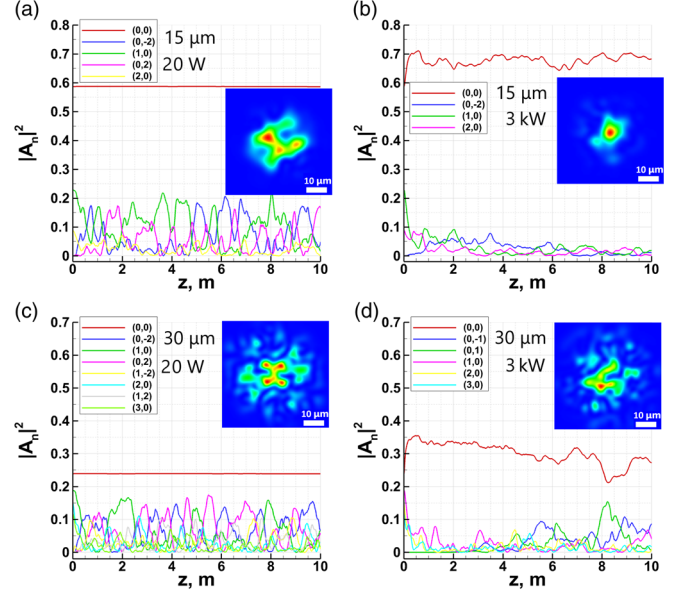FIG. 2.   Evolution of mode intensities with fiber length at low ($P = 20$ W, left) and high ($P = 3$ kW, right) beam powers for 15 μm (a),(b) and 30 μm (c),(d) input beam radius. Insets— corresponding output intensity pattern.

separatrix trajectory (with $q = q_{1\mathrm{crit}} = 1 + K_1 - 2K_2$) divides the phase plane in two regions with an opposite sense of rotation of the phase θ. The separatrix emanates from the saddle point (outer circle, points with $\eta = 1$) and reaches values of $\eta \simeq 0$ before asymptotically (i.e., for large distances) returning to the outer circle. In real world quantities, the threshold for spatial beam cleaning is $p = 32\pi D/q_{1\mathrm{crit}}$, or $P = 32\pi P_{sf}\lambda/2n_0 q_{1\mathrm{crit}} L_B \sim 10$ kW.

Parametric instability leads to a strong dependence of the spatial mode coupling process upon the input beam launching conditions into the MMF. Figure 1 shows that in linear conditions (i.e., with $q = 4$) there are only small intensity oscillations of the fundamental mode as the input conditions are changed. Whereas in the presence of the parametric instability (see Fig. 1, with $q = 0.5$), there is a divergence of the flux of energy in and out of the fundamental mode, whenever input conditions are slightly modified. In addition, the analysis of solutions of Eqs. (5) shows that self-cleaning should be accompanied by depletion of the intermediate mode, so that energy flows into both the fundamental and the high-order mode (see discussion of Fig. 2 of the Supplemental Material [20] for details).

This behavior can be extended to any triplets of modes, say A_0, A_2, A_4 or A_1, A_2, A_3. If the amplitude of the mode with largest wave number is small, its intensity will be increased during the propagation in a GRIN fiber, alongside the increase of amplitude of the mode with the smallest wave number. This results in a transfer of energy to transversal modes with large wave numbers, together with the accumulation of energy in the mode with the smallest wave number (fundamental mode). When taking into account the conservation laws,

$$\sum_{n=0}^{\infty} f_n = 1, \qquad f_n = \sum_{p,m} |B_{p,m}|^2 \delta(n - 2p - |m|),$$

$$\sum_{n=0}^{\infty} n f_n = \bar{n} = \mathrm{const}, \qquad (6)$$

one obtains that if the amplitude of modes with the largest wave number is increased, this means that the amplitude of modes with intermediate wave numbers should decrease. At the same time, the fundamental mode intensity must also grow. In the process, the average mode number is conserved, as predicted by Eqs. (6). This conservation also occurs in the presence of random mode coupling, as long as its spatial correlation length is much longer than the self-imaging period ($\simeq 0.6$ mm, [6]) in the GRIN fiber. The situation is fully analogous to that of 2D turbulence, which exhibits two conservation laws: energy $E = \sum_v \vec{V}_k^2$, and helicity $H = \sum_v \vec{k}^2 \vec{V}_k^2$. In hydrodynamic 2D turbulence, a direct cascade of helicity to large mode numbers (viscous range) is accompanied by the inverse cascade of energy to the fundamental mode (condensate). At the end of the FWM cascade process, one should see the emergence of two spatial scales in the output beam: a condensate (very narrow fundamental mode) and a bottom layer (large number of HOMs with small amplitude), as it was predicted by a statistical study of Aschieri et al. [13].

To confirm our analytical treatment, we performed numerical simulations based on the coupled-mode model (4). The nonlinear coupling coefficients $f_{p,p_1,p_2,p_3}^{m,m_1,m_2,m_3}$ were determined by direct numerical calculation of the corresponding overlap integrals. Coefficients C_{p,p_1}^{m,m_1} correspond to random linear coupling between spatial modes with equal numbers $n = n_1$. In order to preserve the total power, it is necessary that the matrix $C = \{C_{p,p_1}^{m,m_1}\}$ be Hermitian. We consider that only modes with the same mode numbers n are linearly coupled, and that each

element of the matrix C is normally distributed with zero mean and varies randomly during propagation along the fiber with a correlation length of 10 cm. As the initial data, a Gaussian beam of a certain radius was used, which was decomposed into modes, thereby setting the initial modal power distribution. In our simulations, we only consider spatial modes with mode number $n \leq 16$ (153 modes in total).

In Fig. 2(a) we compare the evolution with distance along the fiber of the power in different fiber modes. In quasilinear conditions (input beam power 20 W, Fig. 2(a) for 15 μm beam radius), there is no power exchange between the fundamental mode (solid red curve) and HOMs. However, random mode coupling occurs among all modes except for the fundamental, which leads to an irregular output intensity pattern (top right panel). Whereas for beam powers above the self-cleaning threshold [beam power $P = 3$ kW, Figs. 2(b)], parametric instability first increases the power fraction of the fundamental mode up to about 70% (from 55%) within the first meter of fiber. Next, a continuous energy flow towards HOMs leads to nearly full depletion of intermediate LOMs along the fiber. These properties are better clarified by plotting the corresponding spectra of modal intensities (energy) and of all mode numbers (helicity), respectively, as shown in Fig. 3. As can be seen, above the threshold for spatial beam cleaning ($P = 3$ kW), the LOMs get depleted, and energy flows towards the fundamental mode (inverse cascade) and the HOMs (direct cascade). For a larger beam (30 μm) the effect of self-cleaning becomes much weaker [Figs. 2(c) and 2(d)].

In our experiments, we have verified the analytically and numerically predicted strong sensitivity, induced by the presence of a parametric instability, of beam self-cleaning upon variations of the input beam launching conditions (e.g., the input beam size, or the number of initially excited modes). We launched into a 10-m-long MMF laser pulse from a Q-switched microchip Nd:YAG laser (Standa model STA-01-7), with a duration of 0.6 ns at the wavelength of 1064 nm. Using a 62.5 μm core GRIN fiber, in combination with a beam expander (Standa model 10BE03

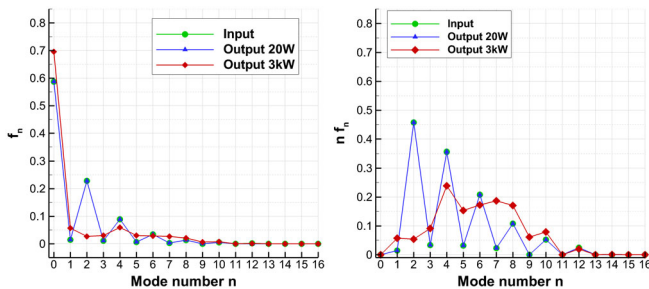diffraction-limited Galilean type beam expander) that allowed us for a continuous change of the input beam radius from 15 to 32 μm, we found that both the establishment and the stability of the self-cleaning effect are strongly dependent of the initial beam parameters, as our theory predicts.

A critical parameter for the observation of stable self-cleaning is the beam size at the fiber input. For an input transverse beam size which is much larger than the diameter of the fundamental mode of the GRIN MMF leads to huge coupling losses, as too many HOMs are excited. When the input beam size is small enough, one excites a beam close to the fundamental mode of the fiber (of ~10 μm radius). Under such conditions, the output beam maintains a good quality, almost independently of power. The most interesting case corresponds to an intermediate beam size, which is close to the condition for optimal energy coupling into the MMF, and still it remains substantially larger than the fundamental mode. In Fig. 4 we illustrate typical cases for the power dependence of the output beam intensity pattern from the GRIN MMF. As can be seen, by increasing the input beam radius from 17 up to 30 μm (correspondingly, the beam coupling efficiency drops from 90% to 55%) while keeping the output peak power stable at 3 kW, the beam self-cleaning effect is totally suppressed, in accordance with theoretical predictions of Figs. 2(c) and 2(d). Whereas, for an input beam radius between 15 and 17($\pm$1) μm, the speckled structure observed at low powers transforms, at powers > 1 kW, into a bright spot (Fig. 4) that is totally insensitive to fiber
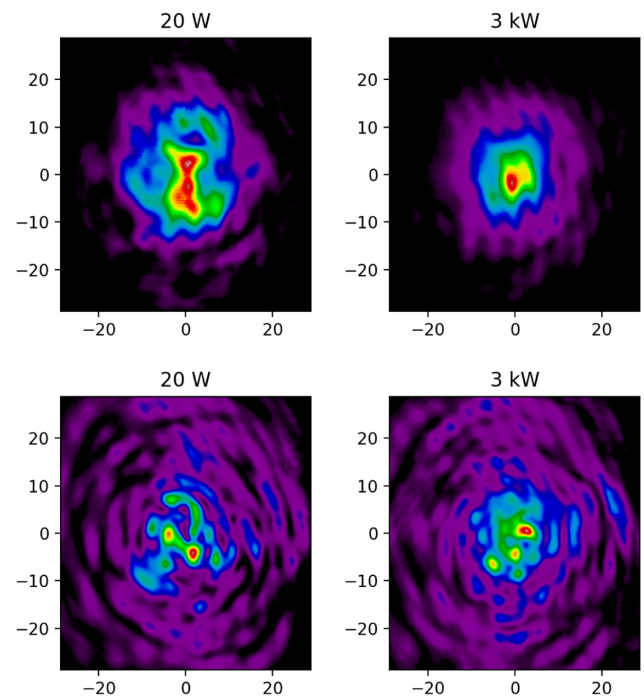

FIG. 3. Evolution with fiber length of mode intensities f_n and helicities $n f_n$ at low ($P = 10$ W) and high ($P = 3$ kW) powers for 15 μm beam radius.

FIG. 4. Experimental output intensity far field patterns for 17 ± 1 μm (top) and 30 μm (bottom) size input beams.

deformations, and changes of the input beam polarization state [7]. Here the input beam radius is measured at the intensity level of $1/e^2$ from the peak.

Our main result is the experimental confirmation of the conservation of the average mode number, as predicted by Eqs. (6), in the process of beam self-cleaning. This condition characterizes the simultaneous occurrence of inverse and direct energy cascade in hydrodynamic 2D turbulence [15,16]. In the experiment, we measure the average mode number as

$$\bar{n} + 1 = \frac{1}{2}\left(\frac{S_{\mathrm{NF}}}{S_{\mathrm{NF}}^0} + \frac{S_{\mathrm{FF}}}{S_{\mathrm{FF}}^0}\right) = \frac{\int r^2 |A(r)|^2 d\vec{r} + \int |\vec{\nabla}A|^2 d\vec{r}}{2\int |A(r)|^2 d\vec{r}},$$

(7)

where S^0 is the area of the fundamental mode, whereas S_{NF}, S_{FF} denote the beam area in near field and far field, respectively. The S^0 value in the near- and far-field was calculated by using the $ABCD$ matrix method, in order to normalize integrals in the equation for the average mode number. The theoretically calculated size of the fundamental mode for a 62.5 μm core GRIN fiber was used as initial value. As a result, we were able to calculate the magnification factor in both cases. In Fig. 5 we show the measured dependence of the average mode number on output peak power for the two cases of 17 ± 1 μm (top) and 30 μm (bottom) size input beams. As can be seen, the input average mode number is conserved in all cases, in excellent agreement with the theoretical values (solid curves). Note that the total number of modes in the GRIN MMF is equal to $M = (n+1)(n+2)/2$. Therefore, our experiments confirm that the mechanism of self-cleaning is based on a mode redistribution from intermediate transversal modes to the fundamental (inverse cascade), and to higher-order ones (direct cascade), as in hydrodynamic 2D turbulence. Such a behavior is associated with the presence of a parametric spatial instability in the nonlinear mode coupling process.
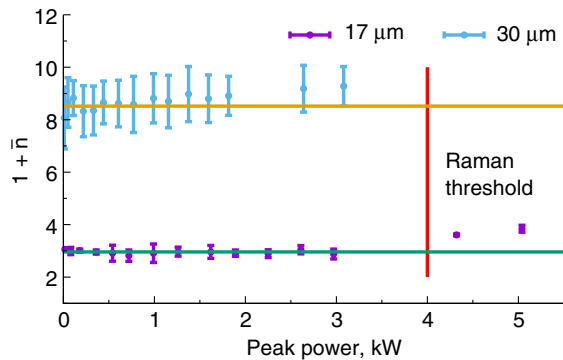
To summarize, we experimentally demonstrated that beam self-cleaning in multimode optical fibers is a process that conserves the average mode number, in spite of the dramatic nonlinear change and self-organization into the fundamental mode of the output intensity pattern. The process of energy flow into the fundamental and HOMs at the expense of modes with intermediate wave numbers originates from a parametric instability, in analogy with hydrodynamic 2D turbulence. These results provide yet another demonstration of the parallelisms between hydrodynamic and optical turbulence, and of the universality of mechanisms for spatial pattern generation in different physical settings.

FIG. 5. Experimental output (dots) and input (solid curves) dependence of the average mode number [from Eq. (7)] vs output peak power, for 17 ± 1 μm and 30 μm size input beams.

[1] L. G. Wright, D. N. Christodoulides, and F. W. Wise, Nat. Photonics 9, 306 (2015).
[2] L. G. Wright, S. Wabnitz, D. N. Christodoulides, and F. W. Wise, Phys. Rev. Lett. 115, 223902 (2015).
[3] A. Hasegawa, Opt. Lett. 5, 416 (1980).
[4] S. Longhi, Opt. Lett. 28, 2363 (2003).
[5] W. H. Renninger and F. W. Wise, Nat. Commun. 4, 1719 (2013).
[6] K. Krupa, A. Tonello, A. Barthélémy, V. Couderc, B. M. Shalaby, A. Bendahmane, G. Millot, and S. Wabnitz, Phys. Rev. Lett. 116, 183901 (2016).
[7] K. Krupa, A. Tonello, B. M. Shalaby, M. Fabert, A. Barthélémy, G. Millot, S. Wabnitz, and V. Couderc, Nat. Photonics 11, 237 (2017).
[8] Z. Liu, L. G. Wright, D. N. Christodoulides, and F. W. Wise, Opt. Lett. 41, 3675 (2016).
[9] L. G. Wright, Z. Liu, D. A. Nolan, M.-J. Li, D. N. Christodoulides, and F. W. Wise, Nat. Photonics 10, 771 (2016).
[10] G. Lopez-Galmiche, Z. S. Eznaveh, M. A. Eftekhar, J. A. Lopez, L. G. Wright, F. Wise, D. Christodoulides, and R. A. Correa, Opt. Lett. 41, 2553 (2016).
[11] K. Krupa, C. Louot, V. Couderc, M. Fabert, R. Guenard, B. M. Shalaby, A. Tonello, D. Pagnoux, P. Leproux, A. Bendahmane, R. Dupiol, G. Millot, and S. Wabnitz, Opt. Lett. 41, 5785 (2016).
[12] K. Krupa, A. Tonello, V. Couderc, A. Barthélémy, G. Millot, D. Modotto, and S. Wabnitz, Phys. Rev. A 97, 043836 (2018).
[13] P. Aschieri, J. Garnier, C. Michel, V. Doya, and A. Picozzi, Phys. Rev. A 83, 033838 (2011).
[14] J. Lægsgaard, Opt. Lett. 43, 2700 (2018).
[15] R. H. Kraichnan, Phys. Fluids 10, 1417 (1967).
[16] R. H. Kraichnan and D. Montgomery, Rep. Progr. Phys. 43, 547 (1980).

[17] C. Milián, V. Jukna, A. Couairon, A. Houard, B. Forestier, J. Carbonnel, Y. Liu, B. Prade, and A. Mysyrowicz, J. Phys. B **48**, 094013 (2015).

[18] B. Prade, M. Franco, A. Mysyrowicz, A. Couairon, H. Buersing, B. Eberle, M. Krenz, D. Seiffer, and O. Vasseur, Opt. Lett. **31**, 2601 (2006).

[19] G. Cappellini and S. Trillo, J. Opt. Soc. Am. B **8**, 824 (1991).

[20] See Supplemental Material at http://link.aps.org/supplemental/10.1103/PhysRevLett.122.103902 for details on the truncated model involving nonlinear coupling among three transversal modes.